# Time Reversal in Wireless Communications: A Measurement-Based Investigation

Hung Tuan Nguyen, *Student Member, IEEE*, Jørgen Bach Andersen, *Life Fellow, IEEE*, Gert Frølund Pedersen, Persefoni Kyritsi, *Member, IEEE*, and Patrick Claus Friedrich Eggers, *Member, IEEE*

***Abstract*— Interference caused by other users in a multi-user environment degrades the system performance significantly. Conventionally, user separation in a multi-user environment is achieved by signal separation in time, frequency or code. The use of multiple elements antenna (MEA) systems can apply separation of the users in space by targeting the transmitted power to the user of interest. Inevitably in that case, the separation is not ideal and there is interference on the other users in the systems. Moreover in a wideband transmission, frequency selective fading causing inter symbol interference (ISI) is a big challenge for point to point wireless communications. In this paper, we study the feasibility of applying the time reversal technique (TR) in multiple input single output (MISO) systems to alleviate the effect of ISI. The ability of TR to focus the signal on the receiver of interest in a multi-user environment is also considered. The studies are supported by measured complex channel impulse responses with 10MHz bandwidth centered at 2.14GHz. For an 8x1 MISO system, using TR the root mean square delay spread is reduced by a factor of 2. To evaluate the capability of the TR in reducing the ISI, simulation of the Bit Error Rate (BER) was made. The irreducible BER of the TR-MISO system was shown to be lower than that of the SISO system by at least an order of magnitude. By using TR and assuming that two users are communicating simultaneously with the same BS the two signals have 17dB of isolation.**

***Index Terms*— Time reversal technique, multiple elements antenna, MISO system, spatial focusing, RMS delay spread, interferences reduction.**

## I. Introduction

TIME REVERSAL (TR) has been a subject of study for some time in acoustic and medical applications (e.g. [1], [2] among others). The main purpose of TR in such applications is to focus energy in space and time on the point of interest by filtering the signal through the complex conjugate and time inverted channel impulse response. TR technique is able to offer fine focusing resolution even in high-order multiple scattering [3]. This occurs robustly despite the fading of the original channel impulse response. Simultaneously, the temporal side-lobes are reduced as the delayed multipath components are added randomly in phase. Therefore the effect of ISI can be alleviated. Nevertheless, there are two requirements for TR to work properly: the channel must be known at the transmitter and must be static during the transmission period.

The use of multiple element antenna (MEA) systems in wireless communications has recently become a well-known technique to increase the transmission reliability and channel capacity. Antenna and diversity gain can be achieved using available combining methods (selection, equal gain, maximum ratio combining). However, for wideband MEA systems where signals are mixed both in time and space a combination of advanced signal processing algorithms such as STBC-OFDM (Space Time Block Code and Orthogonal Frequency Division Multiplexing) or SVD-OFDM (Singular Value Decomposition and Orthogonal Frequency Division Multiplexing) is required to overcome the effect of multipath fading and ISI. Therefore, the receiver is expected to have a rather high complexity. Since the setup of MEA systems has some similarity to TR, it becomes an interesting question whether TR can be applied in MEA wireless systems. If this is the case the advantages will be three fold: i) reducing ISI without the use of an equalizer and ii) focusing the signal on the point of interest thereby reducing the interference iii) applying a rather simple receiver structure.

Due to its simplicity and promising performance improvement, research on the applicability of TR in wireless communication has begun to gain attention. In [4] and [5], using the data from a fixed wireless 8x1 multiple input single output (MISO) measurement a delay compression by a factor of 3 was shown to be possible. Using the reverberant chamber in [6] the convergence of the time-reversed electromagnetic wave to the initial source was illustrated. In [7], transmission of two simultaneous channels at the same frequency in a multipath indoor environment at 2.45GHz was demonstrated. In [8], channel hardening and temporal focusing were observed for ultra wideband signals in an indoor environment.

In this paper the spatial focusing and ISI reduction advantages of TR in a wireless MISO system are investigated. A thorough investigation is presented which gives more physical insight into the working principle of TR than the initial investigation by the same authors in [9]. The studies are supported by measured complex channel impulse responses with 10MHz bandwidth centered at 2.14GHz. The paper is organized in the following way. In Section II we review the transmission technique used in TR. Next, a model for the estimation of the mean signal to interference ratio (SIR) is derived in Section III. Various factors which affect the SIR values are also discussed is the same section. Based on the

Manuscript received November 27, 2004; revised June 2, 2005; accepted July 22, 2005. The associate editor coordinating the review of this paper and approving it for publication was R. Murch. This work was supported by Aalborg University under the Phd Fellowship grant.

The authors are with the Department of Communication Technology, Aalborg University, Niels Jernes Vej 12, DK-9220 Aalborg, Denmark (e-mail: {htn,jba,gfp,persa,pe}@kom.auc.dk).

Digital Object Identifier 10.1109/TWC.2006.04807

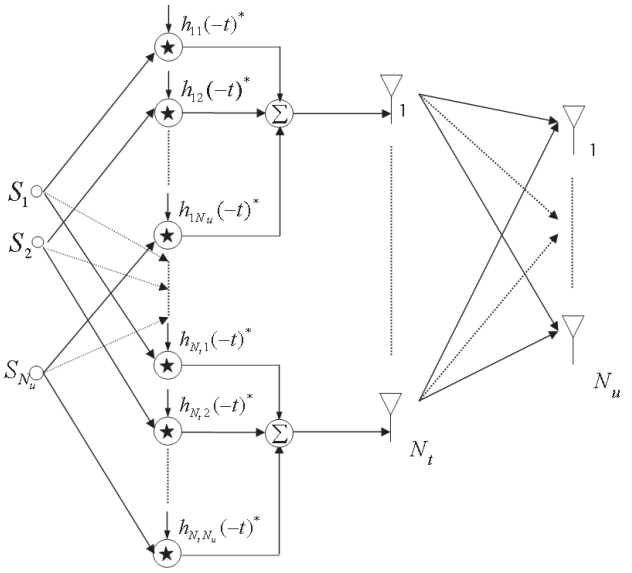


Fig. 1. A transmission approach for multi-user MISO system using TR.

outdoor MISO measurement data, we evaluate the potential benefits from the use of TR in Section IV. The capability to reduce the ISI effect is analyzed by means of the root mean square (RMS) delay spread and the Bit Error Rate (BER). We assess the spatial focusing perspective of TR in MISO systems in terms of the SIR. In Section V a comparison between the TR technique and the eigen beamforming technique with respect to the practical implementation and the spatial focusing performance is presented. The paper ends with conclusions and future work in Section VI.

## II. Time Reversal Technique and Spatial Focusing Quantification

The TR technique requires two steps. First the channel impulse response (IR) is estimated and recorded at the transmit side. Second the desired transmitted symbol is convolved with the complex conjugate of the time reversed version of the IR(s). As long as the channel IRs are known at the transmitter and the channel is static during the transmission period, the actual transmitted signal is convolved with the same IR(s). The result is equivalent to a convolution of the transmitted symbol with the autocorrelation of the channel impulse response as in equation (1)

$$\begin{aligned} y_j(t) &= x_j(t) \star h_{ij}(-t)^* \star h_{ij}(t) + n_j(t) \\ &= x_j(t) \star R_{ij}^{auto}(t) + n_j(t) \end{aligned} \quad (1)$$

where $x(t)$ denotes the transmitted signal and $y(t)$ indicates the received signal; $\star$ denotes the convolution operator; $()^*$ is the complex conjugate operator; $i$ and $j$ are the indices of the transmitting antenna and receiving antenna respectively; $n_j(t)$ is the noise component; $R^{auto}(t)$ is the autocorrelation of the channel IR $h_{ij}(t)$. The received signal at an off-target point has the form

$$x_j(t) \star h_{ij}(-t)^* \star h_{ik}(t) + n_k = x_j(t) \star R_{ijk}^{cross}(t) + n_k(t) \quad (2)$$

where $h_{ik}(t)$ denotes the IR of the channel from the transmitting point to the off-target point and $R_{ijk}^{cross}(t)$ is the cross correlation of the channel IR $h_{ik}(t)$ to the target point and the IR $h_{ij}(t)$.

Let us consider a multi-user MISO system that applies the TR technique. The system comprises $N_u$ simultaneously operating $N_t \times 1$ MISO systems, each one targeting a different user. The signals, before being radiated by the $N_t$ transmitting antennas, are filtered by the corresponding conjugated time reversed impulse responses as described above. The proposed transmission scheme using TR in a wireless multi-user MISO system is sketched in Fig. 1.

The signal received by the $j^{th}$ user can be described as

$$\begin{aligned} y_j(t) &= \underbrace{x_j(t) \star \sum_{i=1}^{N_t} R_{ij}^{auto}(t)}_{S(t)} \\ &+ \underbrace{\sum_{i=1}^{N_t} \sum_{k=1;k\neq j}^{N_u} x_k(t) \star R_{ikj}^{cross}(t)}_{IF(t)} \\ &+ \underbrace{n_j(t)}_{Noise} \end{aligned} \quad (3)$$

where $S(t)$ is the signal of interest and $IF(t)$ is the interfering signal. In the following we use the term "*equivalent channel IR, $h^{eq}$*" to denote the sum of the autocorrelation $R_{ij}$ in equation (3).

$$h^{eq}(t) = \sum_{i=1}^{N_t} R_{ij}^{auto}(t) \quad (4)$$

Under certain conditions, the interference term $IF_j(t)$ in equation (3) becomes comparable to the signal of interest. Correlated IRs caused by closely placed antennas might be one of the reasons. A large number of interference paths compared to the signal of interest, or branch power differences among the receiving antennas might also contribute to this issue. One way to alleviate the influence of the branch power difference is to normalize the time-reversal filter by the square root of its power such as

$$h_{ij}^{TR}(t) = \frac{h_{ij}(-t)^*}{\sqrt{\int |h_{ij}(t)|^2}} \quad (5)$$

This scheme, which we denote as a power control scheme, appears to be practical for the implementation of TR in MEA systems.

From a wireless communication point of view, the spatial focusing capability of TR can be defined by how much the interference from other users can be mitigated. This interference comprises the signals destined for antennas other than the antenna of interest. The spatial focusing potential is characterized by the SIR. The instantaneous SIR is calculated as the ratio of the peak power of $S(t)$ and $IF(t)$.

$$SIR = \frac{|S(t)_{peak}|^2}{|IF(t)_{peak}|^2} = \frac{P_S}{P_{IF}} \quad (6)$$

This SIR is a numerical value for quantifying the capability of TR to focus the transmitted energy into a point of interest: the higher the SIR value the better the focusing resolution. Here we assume that synchronization is established so that we can

always sample precisely at the peak where the received signal contains most of the energy. For simplicity in the calculation of SIR we neglect the side lobe effect caused by the tails of other received symbols at the neighbouring time slots.

## III. A Simple Calculation of the Mean SIR

In this section we derive a simple expression for the mean value of the instantaneous SIR defined in equation (6). It is approximated by the ratio of the mean signal power at the peak of the *equivalent channel IR* and the mean of the interference power at the same time lag. In order to develop an analytical expression, hereafter we only consider the discrete time signals. In the derivation process we assume i) The channel coefficient at the $l^{th}$ tap of the IR is an independent complex number with the real and imaginary parts having zero mean and variance $0.5\sigma_l^2$. Consequently, the magnitude of the tap is Rayleigh distributed, ii) Different taps of the IR are statistically independent (uncorrelated scattering), iii) The channel coefficients between two IRs at the same tap index are mutually uncorrelated. With these assumptions the expected value of the interference power can be calculated as

$$\begin{aligned}\overline{P_{IF}} &= \left\langle \left| \sum_{i=1}^{N_t} \sum_{k=1,k\neq j}^{N_u} \sum_{l=1}^{L} x_k h_{ij}(l) h_{kj}(l)^* \right|^2 \right\rangle \\ &= \sum_{i=1}^{N_t} \sum_{k=1,k\neq j}^{N_u} \sum_{l=1}^{L} |x_k|^2 \sigma_l^4 \\ &= P_o N_t (N_u - 1) \sum_{l=1}^{L} \sigma_l^4 \\ &\leq P_o N_t (N_u - 1) \left( \sum_{l=1}^{L} \sigma_l^2 \right)^2 \end{aligned} \tag{7}$$

where $\langle\rangle$ denotes the expectation operator and $P_o = < |x_k|^2 >$.

The expected value of the signal power is

$$\begin{aligned}\overline{P_S} &= \left\langle |x_j|^2 \left| \sum_{j=1}^{N_t} \sum_{l=1}^{L} h_{ij}(l)^* h_{ij}(l) \right|^2 \right\rangle \\ &= P_o \left\langle \left( \sum_{j=1}^{N_t} \sum_{l=1}^{L} |h_{ij}(l)|^2 \right)^2 \right\rangle \\ &= P_o \left( N_t \sum_{l=1}^{L} \sigma_l^4 + {N_t}^2 \left( \sum_{l=1}^{L} \sigma_l^2 \right)^2 \right) \end{aligned} \tag{8}$$

In the derivation of the signal power above we used the fact that the fourth moment of a zero-mean complex Gaussian is twice the variance squared. From equations (7) and (8) the average SIR can be approximated as

$$\begin{aligned}\overline{SIR} &= \frac{\overline{P_S}}{\overline{P_{IF}}} \\ &= \frac{P_o (N_t \sum_{l=1}^{L} \sigma_l^4 + N_t^2 \left( \sum_{l=1}^{L} \sigma_l^2 \right)^2)}{P_o N_t (N_u - 1) \left( \sum_{l=1}^{L} \sigma_l^4 \right)} \\ &= \frac{1}{N_u - 1} + \frac{N_t \left( \sum_{l=1}^{L} \sigma_l^2 \right)^2}{(N_u - 1) \sum_{l=1}^{L} \sigma_l^4} \\ &\geq \frac{1 + N_t}{N_u - 1} = SIR_{BF} \end{aligned} \tag{9}$$

In equation (9), equality occurs if the channel is narrowband and therefore the channel can be described by a single tap. This means that all the later echoes have almost zero power and, as a result, become insignificant ($\sigma_l^2 \simeq 0$ for $l > 1$). In this case the SIR is essentially a result of the beamforming at the transmit side and henceforth denoted as $SIR_{BF}$.

The derivation of equation (7) and (8) reveals two factors needed to get the best obtainable performance in spatial focusing i) the channel IRs must be uncorrelated so that the interference power is minimized ii) the IRs must have enough significant late echoes to focus the signal in time, therefore maximizing the signal power.

Equation (9) only gives us a lower bound of the mean SIR for the situation when the channel is narrowband and the IRs are uncorrelated. This lower bound is also the SIR obtained by beamforming or maximum ratio combining of the main tap of the IRs. A more exact value of the mean SIR for wideband uncorrelated IRs can be derived if the power variance of the IR taps, $\sigma_l^2$, is known. For an urban environment, the power delay profile (PDP) can be modelled as an exponential decay [10]. The mean power at the $l^{th}$ tap of the PDP can be described by

$$\sigma_l^2 = exp\left( -\frac{(l-1)\Delta\tau}{\overline{\sigma_\tau}} \right) \tag{10}$$

where $\overline{\sigma_\tau}$ is the mean RMS delay spread measured over a particular area and $\Delta\tau$ is the tap resolution.

Applying (10) in (7), the interference power becomes

$$\begin{aligned}\overline{P_{IF}} &= \sum_{i=1}^{N_t} \sum_{k=1,k\neq j}^{N_u} \sum_{l=1}^{L} |x_k|^2 \sigma_l^4 \\ &= P_o N_t (N_u - 1) \left( \frac{1 - exp\left(-\frac{2L\Delta\tau}{\overline{\sigma_\tau}}\right)}{1 - exp\left(-\frac{2\Delta\tau}{\overline{\sigma_\tau}}\right)} \right) \end{aligned} \tag{11}$$

Using (10) in (8), the signal power can be described by

$$\begin{aligned}\overline{P_S} &= P_o \left( N_t \sum_{l=1}^{L} \sigma_l^4 + N_t^2 \left( \sum_{l=1}^{L} \sigma_l^2 \right)^2 \right) \\ &= P_o \left( N_t \frac{1 - exp\left(\frac{-2L\Delta\tau}{\overline{\sigma_\tau}}\right)}{1 - exp\left(\frac{-2\Delta\tau}{\overline{\sigma_\tau}}\right)} + N_t^2 \left( \frac{1 - exp\left(\frac{-L\Delta\tau}{\overline{\sigma_\tau}}\right)}{1 - exp\left(\frac{-\Delta\tau}{\overline{\sigma_\tau}}\right)} \right)^2 \right) \end{aligned} \tag{12}$$

The average SIR changes to

$$\begin{aligned}\overline{SIR} &= \frac{\overline{P_S}}{\overline{P_{IF}}} \\ &= \frac{1}{(N_u - 1)} \left( 1 + N_t \frac{\left( \frac{1 - exp\left(\frac{-L\Delta\tau}{\overline{\sigma_\tau}}\right)}{1 - exp\left(\frac{-\Delta\tau}{\overline{\sigma_\tau}}\right)} \right)^2}{\left( \frac{1 - exp\left(-\frac{2L\Delta\tau}{\overline{\sigma_\tau}}\right)}{1 - exp\left(-\frac{2\Delta\tau}{\overline{\sigma_\tau}}\right)} \right)} \right) \\ &\approx \frac{1}{(N_u - 1)} \left( 1 + N_t \left( 1 + \frac{2exp(\frac{-\Delta\tau}{\sigma_\tau})}{1 - exp(\frac{-\Delta\tau}{\sigma_\tau})} \right) \right) \\ &\quad \text{if } L\Delta\tau \gg \sigma_\tau \end{aligned} \tag{13}$$


Fig. 2. Measurement setup and the map of the three measured routes, handset and measurement scenario (top left), BS and view point from the BS (bottom left), measurement route (right).

From the average SIR expression it can be seen that for the uncorrelated IR case there are three factors which influence the spatial focusing performance of TR. i) The number of transmitting antennas $N_t$. ii) The length of the IR $L\Delta\tau$ when its value is not significantly greater than the delay spread. iii) The product of the bandwidth and the RMS delay spread (effective dispersion) $\frac{1}{\Delta\tau}\overline{\sigma_\tau}$. All these factors indirectly result from the differences in the scattering medium which the signals experience.

Equation (13) is an approximation of the SIR when applying TR for the uncorrelated IR case. However, both the beamforming and temporal focusing contribute to the spatial focusing performance of TR. From equations (9) and (13) the contribution of the temporal focusing in TR can be easily separated as

$$\begin{aligned}\overline{SIR}_{TF} &= \frac{SIR}{SIR_{BF}} = \frac{1}{N_t+1}\left(1+N_t\frac{\left(\frac{1-exp\left(-\frac{L\Delta\tau}{\sigma_\tau}\right)}{1-exp\left(-\frac{\Delta\tau}{\sigma_\tau}\right)}\right)^2}{\left(\frac{1-exp\left(-\frac{2L\Delta\tau}{\sigma_\tau}\right)}{1-exp\left(-\frac{2\Delta\tau}{\sigma_\tau}\right)}\right)}\right) \\ &\approx \frac{1+N_t\left(1+\frac{2exp(-\frac{\Delta\tau}{\sigma_\tau})}{1-exp(-\frac{\Delta\tau}{\sigma_\tau})}\right)}{N_t+1} \text{ if } L\Delta\tau \gg \sigma_\tau \qquad (14)\end{aligned}$$

## IV. Evaluation of Dispersion Reduction and Spatial Focusing Based on Measurement Data

### A. Measurement Setup and the Environment

The data used for the evaluation was acquired from wideband outdoor 8x4 MIMO measurements in Aalborg, an urban environment with hilly terrain, along three different routes of length 1 km each (4400x8x4 IR(s) per route). The transmitter was a base station (BS) antenna prototype made by ALLGON in Sweden which had 8 antenna outputs, arranged in four dual polarized columns. In the measurement campaign the transmitting antennas were mounted at the fence of a balcony on the 5th floor (rooftop level). The receiver was a prototype of a commercial mobile handset which was battery powered to avoid conductive cables. This handset was equipped with 4 patch antennas at its four corners (labelled as A1, A2, B1, B2 in Fig. 2).

Optical cable was used to connect the handset to the measurement equipment to avoid the radiation perturbation that would have been introduced by a coaxial cable. Four antenna outputs of the handset was multiplexed into 2 parallel channels. Each channel was fitted with an antenna switch so that each vertical antenna pair was selected in turn by a trigger. The switch was followed by a standard UMTS filter and a two step variable gain block. Finally it is connected to the optical transmitter, where the received signals were modulated at an optical carrier, and sent over an optical fibre to the optical receiver. The handset was placed on a trailer pulled by a car which ran at a velocity ranging between 20km/h and 40 km/h. The measurements were taken in a burst mode: the channel was measured along a distance of 2 meters during which 44 IRs were acquired, followed by 8 meters of travelled distance during which no measurements were taken.

The sounding system was based on post-processing and real antenna array gain. A code phase offsetting technique was applied, whereby each antenna element at the transmitter used the same Pseudo random Noise sequence (PN-sequence) code, but it was offset by a predefined interval. Using this technique together with the switching 8x4 channel, IRs can be almost instantaneously measured. In our measurement campaign we used a PN sequence of 511 bits length with the chip rate of 7.665MHz. The tap delay resolution of the system therefore was $0.13\mu$s. This PN sequence was transmitted at the center frequency of 2140MHz corresponding to a carrier wavelength of 14.1 cm. At the receive side, the signal was sampled at a rate of 15.36MHz so there were 1024 samples for one PN sequence length of 511 bits. The center frequency and the measurement bandwidth are comparable to the standard center frequency and bandwidth of 3G WCDMA systems. The carriers at the handset and the BS were synchronized by standard Rubidium oscillators. The instantaneous measurement signal to noise radio, $SNR_m$ for all of the measured data was well beyond 40dB. Although the length of each measured IR was 98 taps by visually inspecting the measured IRs we decided to use only 70 taps since the rest of the taps do not contain much energy and multipath information.

Fig. 2 illustrates the setup of the handset, the transmitting antenna, the viewpoint from the BS as well as the measurement routes in the campaign. In the following assessment of the potential of TR it is assumed that the measured IRs are instantaneously known at the transmitter, and that the channel is static during the period in which a symbol is transmitted.

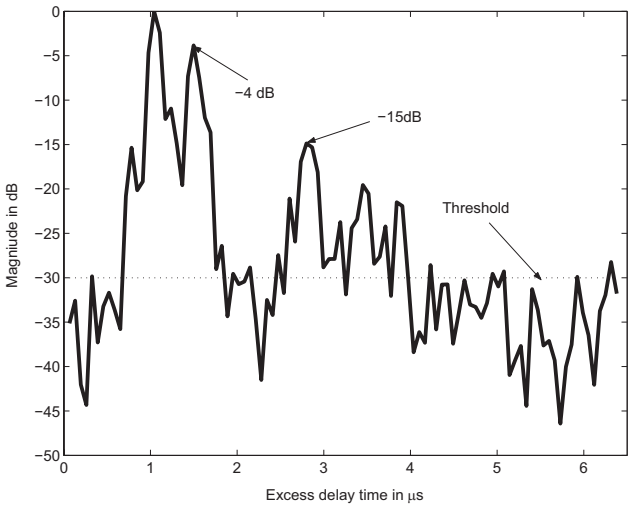


Fig. 3. An example of the channel impulse responses of route 2.

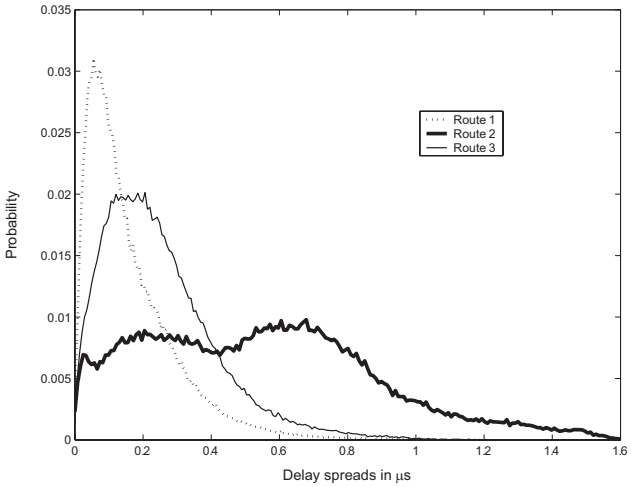


Fig. 4. Probability distribution of the instantaneous RMS delay spread based on the IRs of the three routes.

### B. Dispersion Reduction Capability

As mentioned in Section I, one of the most interesting properties of TR is its capability to reduce ISI. In fact, the advantage of TR in ISI reduction depends strongly on the frequency selective nature of the environment. The more wideband the channel is, the more benefit we can get out of TR in suppressing the delayed echo components. In this section, we investigate this property based on the data from the measurement campaign described in Section IV-A.

First, we consider the frequency selective fading characteristics of the measured environment. Fig. 3 shows an example of the magnitude of a sample channel IR taken from the second route (normalized such that the maximum value is set to 0dB). The IR is composed of a main strong peak and several significant delayed echoes.

Root mean square (RMS) delay spread is a useful parameter to describe the dispersion or the multipath effect of the channel. Depending on the relative magnitude of this parameter with respect to the bandwidth of transmitted signal, the channel can be described as frequency flat or frequency selective. The instantaneous RMS delay spread is calculated from the second central moment of the instantaneous PDP [11]

$$\sigma_\tau = \sqrt{\frac{\sum_{l=1}^{L} PDP(l)\tau_l^2}{\sum_{l=1}^{L} PDP(l)} - \left(\frac{\sum_{l=1}^{L} PDP(l)\tau_l}{\sum_{l=1}^{L} PDP(l)}\right)^2} \quad (15)$$

where $PDP(l) = |h_{ij}(l)|^2$ and $\tau_l$ is the excess time delay. For the calculation of the RMS delay spread, in order to reduce the thermal noise and the correlation noise, a threshold of 30dB is used for the PDP. Those components that are lower than 30dB from the peak are set to zero. The probability distributions of the RMS delay spreads for three routes are shown in Fig. 4.

The mean RMS delay spread is $0.26\mu$s, $0.62\mu$s and $0.34\mu$s for the first, second and third route, respectively. Obviously, $\overline{\sigma_\tau}$ is larger than the delay resolution ($0.13\mu$s) at least by a factor of 2. The delay resolution of the system is capable of resolving the multipath components in the outdoor environment for more than 50% of the measured paths.

Secondly, in order to illustrate the dispersion reduction capability of TR, we concentrate on the *equivalent channel IR*. These autocorrelations are derived from the IRs between the 8 transmitting antennas at the BS and a single receiving antenna at the handset. An example of the autocorrelations and the $h^{eq}(t)$ is shown in Fig. 5.

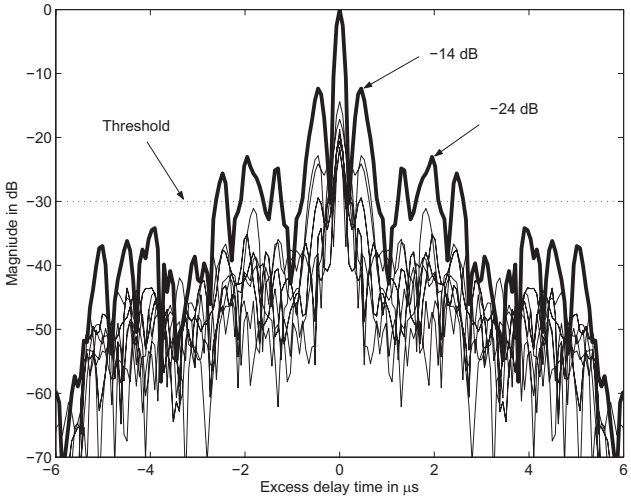


Fig. 5. An example of the $h^{eq}$ or the sum of 8 autocorrelations, bold curve.

By comparing Fig. 3 and Fig. 5 we can see that the later echoes have been suppressed in the *equivalent channel IR* after TR. Without TR, the second highest signal peak is 4dB lower than the peak. With TR the second highest peak is 14dB lower than the peak and therefore the sidelobes have clearly been suppressed.

The RMS delay spread of the *equivalent channel IR* is also calculated in a manner similar to the calculation used for the measured IRs. The channel IR $h_{ij}$ in equation (15) is replaced by the *equivalent channel IR*, $h_j^{eq}$ and the tap index $l$ ranges from 1 to $2L-1$. A threshold of 30dB is also used. The probability density function of the RMS delay spread is illustrated in Fig. 6.

A comparison between the delay spread of the original IRs and that of the *equivalent channel IR* is of interest in order to see how much the channel dispersion has been reduced. Table I compares these mean RMS delay spread values obtained

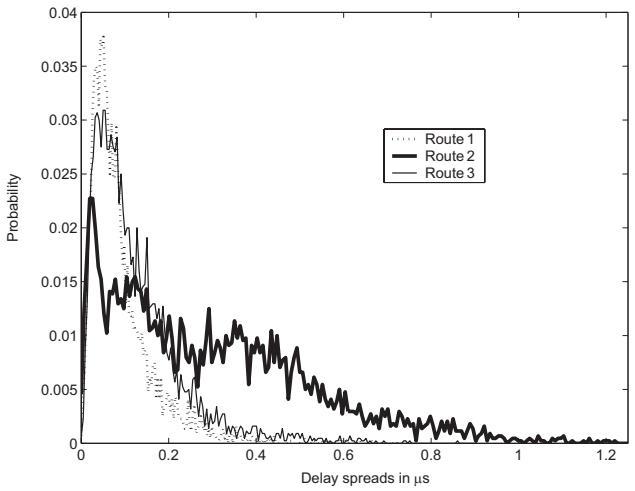


Fig. 6. Probability distribution of the instantaneous RMS delay spread of the *equivalent IR*, $h^{eq}$ in the three routes.

from the three measured routes. The RMS delay spread has been reduced approximately by a factor of 2. The reduction in the mean RMS delay spread values indeed reinforces the conclusion on the ISI reduction capability of TR.

Two observations can be drawn from the above results. i) if the number of transmitting antennas is increased, the ISI effect will be further reduced. This is because in the sum of the autocorrelations, the peaks add up coherently as all components have zero phase here. The side lobes add non-coherently due to independent random phase on all components, and therefore the composite sidelobes are suppressed. ii) if the environment becomes more frequency selective (more delayed echoes), the autocorrelation will be more focused in time and more energy of the signal will be concentrated at the peak of the autocorrelation. Thereby the impact of energy leakage from one symbol to its neighboring symbols will be further alleviated.

For completeness, using the measured data, we made a performance comparison in terms of the bit error rate (BER) obtained by a single user TR-MISO system and a normal single user SISO system without using TR. To highlight the influence of the ISI, no equalizer is used at the receiver. Several guard intervals of G=2, 4, 8 and 16 taps were considered. The closer the symbols are placed the higher the throughput, however it is traded for a higher ISI and a high BER as a result. For the simulation we used a simple binary phase shift keying (BPSK) modulation. The symbol width is assumed to be much smaller than the tap interval so as the convolution of the signal with the *equivalent channel IR* essentially is the multiplication of the *equivalent channel IR*'s tap with the transmitted symbol. Since the tap interval in the measurement was $T_s = 1/15.36MHz = 65.1ns$, the bit rates corresponds to the guard intervals are approximately $\frac{1}{GT_s}$ =7.68Mbps, 3.84Mbps, 1.92MBps and 0.96Mbps.

We assume that the receiver samples the received signal at the instant when the channel impulse response (or the equivalent channel impulse response in the TR case) has the maximum energy. The power of the sampled signal $P_{max}$ is calculated as

TABLE I
MEAN RMS DELAY SPREAD OF THE IRS AND OF THE *Equivalent Channel IRs*

| Route no | $\overline{\sigma_\tau}$ | |
|---|---|---|
| | IRs, $h_{ij}$ | *Equivalent channel IR*, $h_l^{eq}$ |
| 1 | 0.2 $\mu$s | 0.1 $\mu$s |
| 2 | 0.6 $\mu$s | 0.3 $\mu$s |
| 3 | 0.3 $\mu$s | 0.1 $\mu$s |

$$P_{max} = \begin{cases} max\left(|h(l)|^2\right) P_o \text{ , Original IR}, l = 1..L \\ max\left(|h^{eq}(l)|^2\right) P_o \text{ , Equivalent IR } , l = 1..2L-1 \end{cases} \quad (16)$$

where $P_o$ is the transmitted signal power. The sampling instant $L_{sam}$ is defined as

$$L_{sam} = \begin{cases} \text{argmax}_l |h(l)|^2 \text{ , Original IR} \\ \text{argmax}_l |h^{eq}(l)|^2 \text{ , Equivalent IR} \end{cases} \quad (17)$$

Based on this observation, the receiver detects the originally transmitted symbol without performing any equalization.

In our simulations, the original channel IR for the SISO case and the *equivalent channel IR*, $h^{eq}$ for the TR-MISO case are normalized so that their signals have the same total power level $S = \sum_{l=1}^{L} |h(l)|^2 = \sum_{l=1}^{2L-1} |h^{eq}(l)|^2$. In this way the link budget is the same for both SISO and TR-MISO system. Thereby the temporal focusing characteristics of TR is highlighted. We varied the signal to noise ratio (SNR), defined as the ratio of the total received power $S$ to the variance of the additive white Gaussian noise N. We approximate the inter symbol interference as a Gaussian random variable. This simplifying assumption is within 2dB of the true performance for the range of SNRs of interest. Therefore, if we assume BPSK modulated signals, the BER for one channel realization can be estimated as

$$BER = 0.5\text{erfc}\left(\sqrt{\frac{P_{max}}{I+N}}\right) \quad (18)$$

where erfc() is the complementary error function, $P_{max}$ is the power of the sampled signal and $N$ is the noise variance. The expected value of the inter symbol interference power $I$ is calculated as equation (19), which is located on the next page, where G is the guard interval. As mentioned in Section IV-A the number of measured IRs per route was 8x4x4400, therefore for each SNR values there are 8x4x4400 realizations for the BER simulation of the SISO system. Similarly, there are 4x4400 realizations of the 8x1 MISO TR channel, and for each one of them the BER is calculated as in equation (18). The results are then averaged over the whole route.

The performance enhancement due to the use of TR is shown in Fig. 7. At a bit rate of 7.68Mbps the BER floor of the TR-MISO system is always lower than that of the SISO system by an order of magnitude. For the bit rates less than 2Mbps, while the BER of the SISO system reaches a BER floor at some points, the SNR value where the BER floor of the TR-MISO system occurs is out of the observed SNR range. As seen from the RMS delay spread results, the highly

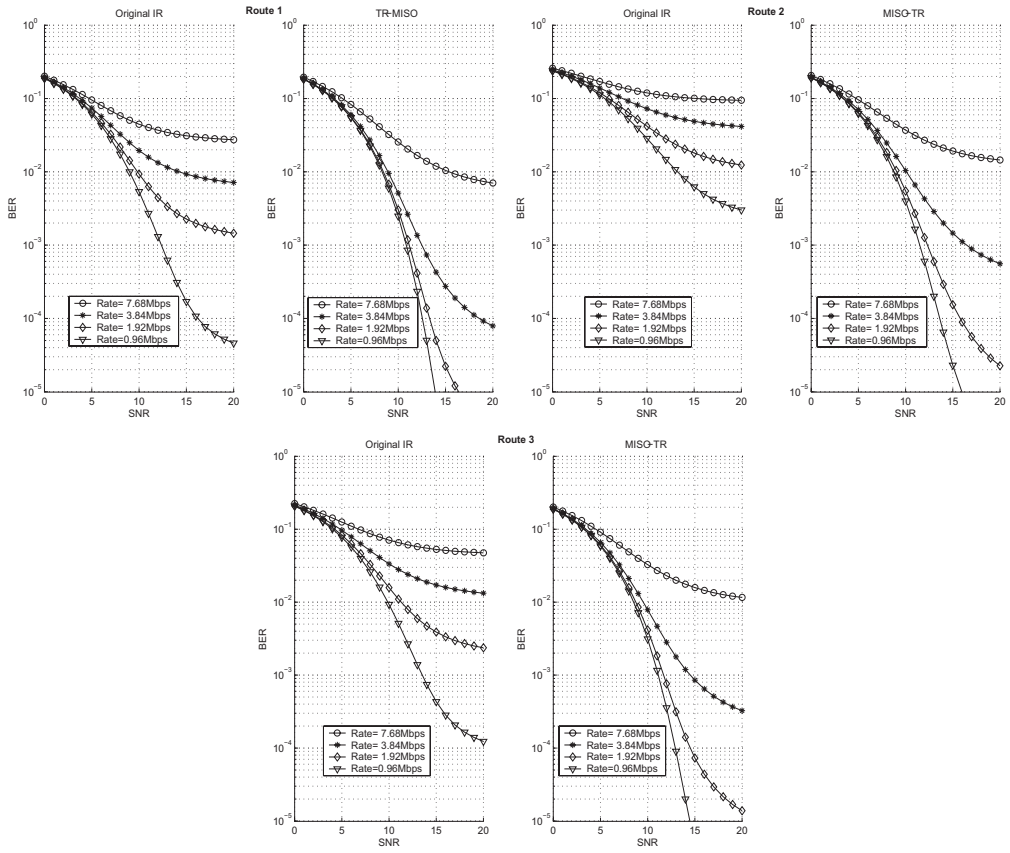


Fig. 7. BER comparisons between the SISO and the TR-MISO systems at different bit rates.

$$I = \begin{cases} P_o \left( \sum_{l=L_{sam}-G}^{l=l-G,l=1} |h(l)|^2 + \sum_{l=L_{sam}+G}^{l=l+G,l=L} |h(l)|^2 \right) & \text{Org IR} \\ P_o \left( \sum_{l=L_{sam}-G}^{l=l-G,l=1} |h^{eq}(l)|^2 + \sum_{l=L_{sam}+G,}^{l=l+G,l=2L-1} |h^{eq}(l)|^2 \right) & \text{Equ IR} \end{cases} \tag{19}$$

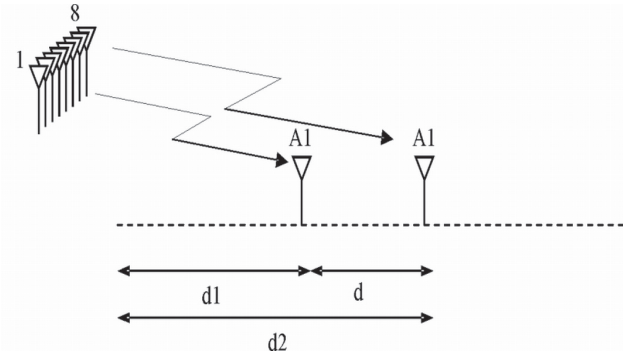


Fig. 8. Illustration of the separation distance between users along the measurement route.

frequency selective characteristic of the environment in the second route leads to a significant difference in the BER of these SISO and TR-MISO systems.

### C. Spatial Focusing

In this section the spatial focusing property of TR in the 8x1 down-link setup is evaluated. The available measured data can be used to mimic a multi-user environment. We consider a simple scenario where there are two users separated by distance $d$. Each user is equipped with a single receiving antenna and both users operate simultaneously. There are still 8 antennas at the transmit side. Eight IRs measured at one location are used to calculated the power of the signal of interest as the numerator in equation (6). From the measurement data, the fading correlation between transmitting antennas was estimated and it is smaller than 0.4 for most of the cases.

The eight other IRs measured at a distance $d$ far apart are used to calculate the interference power as the denominator in equation (6). Illustration of the multi-user scenario and the distance between the users is shown in Fig. 8.

Fig. 9 illustrates the mean of the instantaneous SIR values as a function of the distance between the two users along these three measured routes. The SIR resulting from both schemes, with and without power control, is shown. TR indeed provides a large gain in terms of the SIR in the multi-user scenario. The mean SIR value increases when the distance between the users increases. It saturates when the distance between two users is

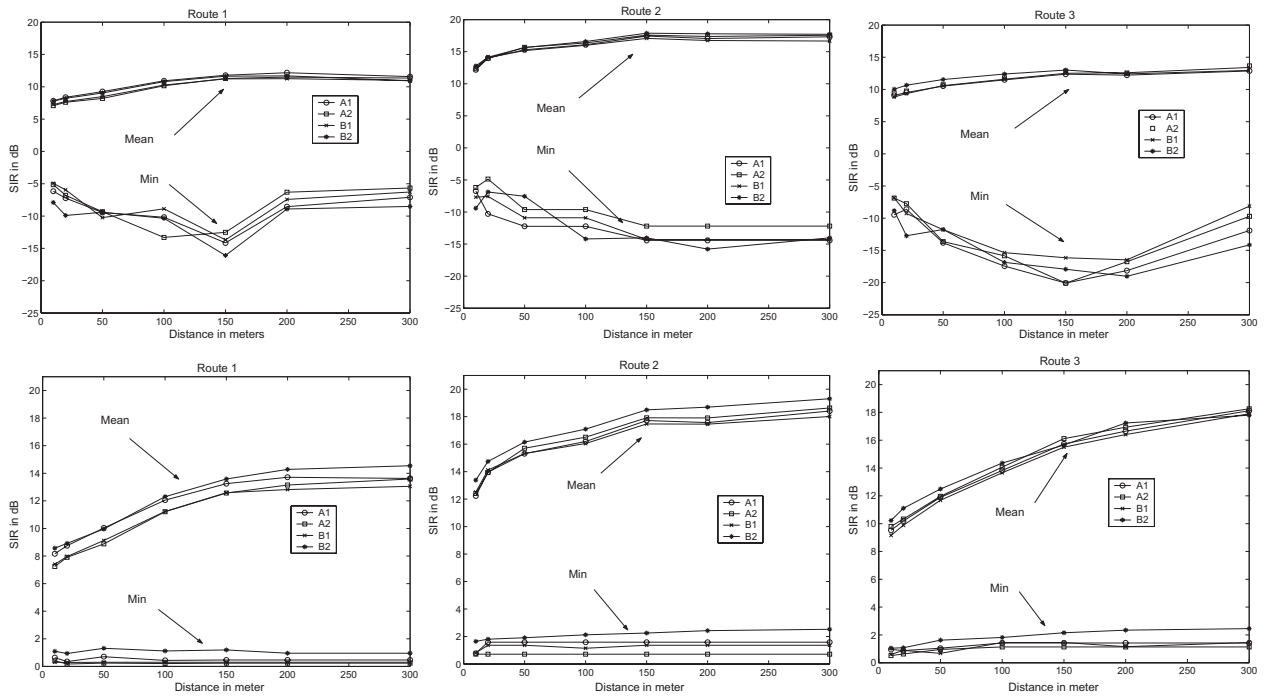


Fig. 9. Maximum, Mean and Minimum value of the SIR vs distance without power control (top row) and with power control (bottom row) for 3 routes.

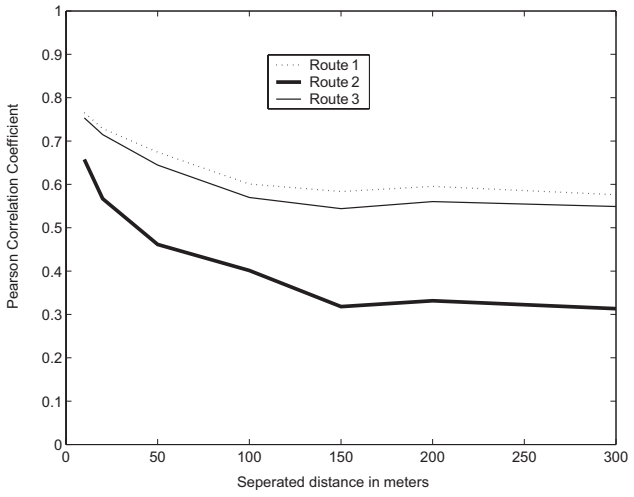


Fig. 10. Pearson's correlation coefficient of two IRs as a function of the separation distance.

above a certain value (i.e. 18 dB at a distance of 300 meters). With power control we get higher SIR, its minimum value for most of the routes is around 1dB. The mean SIR ranges from 8dB to 18dB when the distance between the two users varies from 10 meters to 300 meters.

The estimation in Section III gives us a lower bound of the mean SIR value of 9dB when there are 8 antennas at the transmit side and 2 antennas at the receive side. With the common measured mean RMS delay spread of $\overline{\sigma_\tau} = 0.3\mu s$ the estimated SIR is 18.7dB. The approximation of the mean SIR in Section III was derived under the assumption of uncorrelated IRs. This condition is satisfied when the two receiving antennas are placed far enough apart. When the distance between the two users is around 100 to 300 meters (Fig. 9) there is a good match between the mean of the instantaneous SIR value from the measurements and the approximated mean SIR from the model (17dB and 18.7dB respectively). Following up on equations (9) and (15), it is interesting to see that the beamforming ($SIR_{BF}$) and the temporal focusing of TR ($SIR_{TF}$) have almost equal contributions (i.e. each 9dB) to the overall spatial focusing performance. Therefore this simple model can be used as a guide line for estimating and understanding the potential of TR with respect to its temporal and spatial focusing characteristics.

In an urban environment, it has been confirmed by measurements that the signal arrives in clusters, and clustering of the scatterers leads to an increase in the delay dispersion (e.g. [12], [13] among others). Obviously if two receiving antennas are placed far enough apart (e.g. 200m in our measurement) the IRs to the two users are no longer described by the same Wide Sense Stationary Uncorrelated Scattering (WSSUS) model and they experience independent clusters. This leads to a difference in the shapes of the IRs observed at these two locations. In TR, the interference is calculated as the sum of the cross-correlations of two IRs as stated in equation (2). The difference in the shape of the IRs and the shift in time of their major peaks can lead to a situation where the taps of the TR filter containing significant energy are multiplied by taps of the channel with weak amplitude and vice versa. Thus, decorrelation with respect to the shapes of the IRs can also contribute to the reduction of the interference power, and consequently increase the mean SIR values. To support this conclusion, from the collected data we calculate the correlation of the magnitude of the IRs measured at two different points along the route. We use Pearson's correlation [14] as a means to estimate how similar in shape the magnitudes of the two IRs are. Pearson's correlation is defined in equation (20), which is found at the top of the next page. In this equation $L$ is

$$\rho_{Pearson} = \frac{\sum_{l=1}^{L}(|h_{d_1}(l)| - \overline{|h_{d_1}|})(|h_{d_2}(l)| - \overline{|h_{d_2}|})}{\sqrt{\sum_{l=1}^{L}(|h_{d_1}(l)| - \overline{|h_{d_1}|})^2}\sqrt{\sum_{l=2}^{L}(|h_{d_2}(l)| - \overline{|h_{d_2}|})^2}}; \overline{|h_{d_{1,2}}|} = \frac{\sum_{l=1}^{L}|h_{d_{1,2}}(l)|}{L} \quad (20)$$

the number of taps, subscripts $d_1$ and $d_2$ denote the distance between the measurement location of the IR and the starting point of the measured route. The separation distance between the two points therefore becomes $d = d_2 - d_1$ as in Fig. 8. The correlation $\rho_{Pearson}$ tells us both the strength and the sign of the relationship and is between $-1$ and $+1$. The closer to zero it is the more uncorrelated the two samples.

From Fig. 10 it is apparent that in the first 100m the Pearson correlation of the two IRs depends strongly on the separation distance. It has a declining trend and reaches a floor as the distance between the receiving antennas increases. Interestingly, we observe that both the correlation and the SIR become saturated at the same distance (i.e. 150 meters). This observation highlights the influence of the changes in the shapes of the IRs on the spatial focusing capability of TR. The correlations are also different in the three measured routes. This can also explain the higher SIR values observed along one route relative to the others.

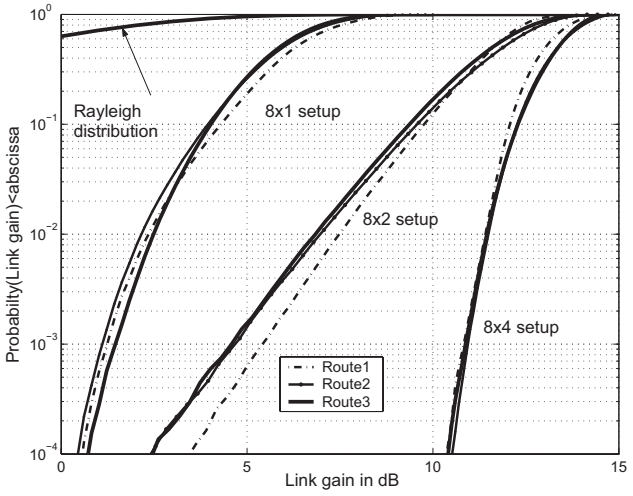


Fig. 11. Link gain obtained by the SVD for 8x1, 8x2 and 8x4 setup of the three routes.

## V. A Comparison on the Spatial Focusing Performance of TR and SVD Techniques

The success of the TR depends heavily on the availability of the IRs at the transmitter. In practice, in order to use TR at both the uplink and the downlink the channel information is needed at the receiver as well. However, from this channel information, other schemes such as Singular Value Decomposition (SVD) transmission can be applied to obtain spatial focusing. We investigate the potential of the maximum eigen beamforming in supporting concurrent independent data channels from the transmit side to $N_u$ users. The issue of frequency selective fading is assumed to be addressed by proper OFDM technique so that the SVD can be applied as if the channel were narrowband (eigen beamforming on a tone-by-tone basis) [15]. The eigenvectors applied at the transmitter and at the receiver act as steering vectors to focus the signal on the intended user. We further assume that the channels experienced by the users are totally uncorrelated, which is a reasonable assumption provided that these users are separated far enough apart. At one frequency tone, the channel matrix of the $k^{th}$ user, $k \subset (1..N_u)$, is denoted as $H_k$. Furthermore, $u_k$ and $v_k$ are the eigenvectors associated with the maximum eigenvalue of $H_k$. The symbol intended for the $k^{th}$ user is denoted as $x_k$ and its corresponding power is $P_o$. At one frequency tone, the received signal of the $j^{th}$ intended user becomes

$$\begin{aligned} y_j &= \underbrace{x_j u_j' H_j v_j}_{S_j} + \underbrace{\sum_{k=1,k\neq j}^{k=N_u} x_k u_k' H_j v_j}_{IF_j} + \underbrace{n_j}_{Noise_j} \\ &= x_j\sqrt{\lambda_{max_j}} + \sum_{k=1,k\neq j}^{k=N_u} x_k u_k' H_j v_j + n_j \end{aligned} \quad (21)$$

where $()'$ denotes the complex transpose operator. Because $u_k$ and $v_j$ are the eigenvectors and if $H_j$ is a matrix with identical independent distributed component with zero mean and unit variance, the interference term in equation (21) is also a random complex number with zero mean and variance equal to $(N_u - 1)P_o$. Hence the average SIR obtained by the maximum eigen beamforming at one arbitrary frequency tone is

$$SIR = \frac{\overline{\lambda_{max}}}{N_u - 1} \quad (22)$$

It is immediately obvious that when there are two concurrent users the SIR can be approximated by the mean of the largest eigenvalue. From the collected data, we calculated the maximum eigenvalues, or the link gain as defined in [16], for different transmitting-receiving antenna setups along each measurement route. The cumulative distribution functions of these link gains are shown in Fig. 11.

The results show that the mean link gain and therefore the mean SIR values are 5.7dB, 11.5dB and 13.6dB for the 8x1, 8x2 and 8x4 setups respectively. Meanwhile, under ideal conditions i.e. assuming that two users are separated far enough apart so that their IRs are uncorrelated, the mean SIR of 8x1 setup using TR is around 17dB. The results illustrate that TR outperforms the SVD technique in the spatial focusing perspective. Concerning the complexity of the system, TR-MISO also outperforms the SVD technique as it only requires a single receiving antenna for each user. Moreover, the SVD technique requires more advanced signal processing algorithm than TR.

Since in TR the ISI can not be mitigated completely, the comparisons mentioned above are somewhat biased in favor of the TR. In addition, with the knowledge of the channel state information at both the link ends, it is possible to have better signal processing algorithms to deal with spatial focusing and

ISI reduction. Nevertheless, through the comparison we have highlighted the advantage of TR concerning its simplicity in the deployment, without compromising the system performance.

## VI. Conclusion

In this paper, the potential of TR has been verified in actual MEA wireless communications. A number of investigations with the data collected from a large outdoor measurement campaign has been carried out. We showed that TR is promising with respect to ISI reduction and its spatial focusing capabilities. Using TR, for the 8x1 setup the mean RMS delay spread is reduced almost by a factor of 2 as compared to the case when no TR is used. This indicates that with the use of TR the receiver can be rather simple. Simulation based on the measured data also shown that the BER floor level due to the ISI effect is reduced significantly when applying TR. In general, the BER floor of the TR-MISO system is always lower than that of the SISO system by at least an order of magnitude. For a lower transmitted bit rate (e.g. smaller than 2Mbps), while the BER of the SISO system reach a floor at some SNR values no BER floor is observed for the MISO-TR system in the SNR range of 0dB to 20dB. For a multi-user scenario, a mean SIR value of around 17dB was found for two concurrent users equipped with single receiving antenna each and 8 transmitting antennas at the BS. This illustrates that using TR can help reduce the interference and the probability of intercept. We presented a simple model for estimating the mean SIR value which can be obtained by the use of the TR technique. The SIR value calculated from the measurements is fairly close to what has been estimated by our model. This is only an initial investigation on the potential of TR under ideal conditions such as perfect knowledge of the instantaneous IR. Nevertheless, the results from this paper can provide useful guidelines for the understanding and the potential deployment of TR in wireless MEA systems. Further investigations include the performance of TR when the transmitting antennas are distributed rather than centralized. In this case, not only are the channel IRs uncorrelated but also the scattering medium observed by transmitting antennas is different. Therefore it is expected that the spatial focusing performance of the TR in that case will improve. A model to estimate the mean SIR when both the complex and the envelope correlations of the IRs are taken into account is an interesting problem for future work. Besides, applying TR in extremely wideband signal such as UWB signals in order to improve the temporal focusing performance could also be an interesting direction [17], [18].

## Acknowledgement

Nokia is kindly acknowledged for their financial contribution and support in the measurement campaign. The authors would like to thank anonymous reviewers for their constructive comments and insights.

## References

[1] M. Fink, "Time-reversed acoustic," *Scientific American*, pp. 67-73, Nov. 1999.

[2] R. K. Ing and M. Fink, "Ultrasonic imaging using spatio-temporal matched field (STMF) processing: Applications to liquid and solid waveguides," *IEEE Trans. Ultrason., Ferroelect., Freq. Contr.*, vol. 48, no. 2, pp. 374-386, Mar. 2001.

[3] A. Derode, P. Roux, and M.Fink, "Acoustic time-reversal through high-order multiple scattering," in *Proc. IEEE Ultrasonics Symposium*, Nov. 1995, vol. 2, pp. 1091-1094.

[4] P. Kyritsi, P. Eggers, and A. Oprea, "MISO time reversal and time compression," in *Proc. URSI International Symposium on Electromagnetic Theory*, May 2004.

[5] P. Kyritsi, G. Papanicolaou, P. Eggers, and A. Oprea, "MISO Time reversal and delay-spread compression for FWA channels at 5 GHz," *Antennas and Wireless Propagation Letters*, vol. 3, no. 6, pp. 96-99, 2004.

[6] G. Lerosey, J. de Rosny, A. Tourin, A. Derode, G. Montaldo, and M. Fink, "Time reversal of electromagnetic waves," *Physical Review Letters*, vol. 92, pp. 193904-1 193904-3, May 2004.

[7] B. E. Henty and D. D. Stancil, "Multipath-enabled super-resolution for RF and microwave communication using phase-conjugate arrays," *Physical Review Letters*, vol. 93, pp. 243904-1 243904-4, Dec. 2004.

[8] S. M. Emami, J. Hansen, A. D. Kim, G. Papanicolaou, A. J. Paulraj, D. Cheung, and C. Prettie, "Predicted time reversal performance in wireless communications using channel measurements," *IEEE Commun. Lett.*, accepted for publication.

[9] H. T. Nguyen, J. B. Andersen, and G. F. Pedersen, "The potential use of time reversal technique in multiple elements antenna systems," *IEEE Commun. Lett.*, vol. 9, no. 1, pp. 40-42, Jan. 2005.

[10] R. Vaughan and J. B. Andersen, *Channels Propagation and Antennas for Mobile Communications (Iee Electromagnetic Waves Series, 50)*. London, UK: Institute of Electrical Engineers, 2003.

[11] T. S. Rappaport, *Wireless Communications, Principles and Practice*. Upper Saddle River, NJ: Prentice Hall PTR, 1996.

[12] A. Kuchar, J. P. Rossi, and E. Bonek, "Directional macro-cell channel characterization from urban measurements," *IEEE Trans. Antennas Propagat.*, vol. 48, no. 2, pp. 137-146, Feb. 2000.

[13] K. I. Pedersen, P. E. Mogensen, and B. H. Fleury. "A stochastic model of the temporal and azimuthal dispersion seen at the base station in outdoor propagation environments," *IEEE Trans. Veh. Technol.*, vol. 49, no. 2, pp. 437-447, Mar. 2000.

[14] R. Russo, *Statistics for the Behavioural Sciences: An Introduction*. Essex, UK: Psychology Press, 2003.

[15] G. L. Stuber, J. R. Barry, S. W. McLaughlin, Y. G. Li, M. A. Ingram, and T. G. Pratt, "Broadband MIMO-OFDM wireless communications," Invited Paper, in *Proc. IEEE*, Feb. 2004, vol. 92, no. 2, pp. 271-294.

[16] J. B. Andersen, "Array gain and capacity for known random channels with multiple element arrays at both ends," *IEEE J. Select. Areas Commun.*, vol. 18, no. 11, pp. 2172-2178, Nov. 2000.

[17] T. Strohmer, M. Emami, J. Hansen, G. Papanicolaou, and P. J. Arogyaswami, "Application of time-reversal with MMSE equalizer to UWB communications," in *Proc. IEEE Global Telecommunications Conference*, Dec. 2004, vol. 5, pp. 3123-3127.

[18] H. T. Nguyen, I. Z. Kovacs, and P. Eggers, "A time reversal transmission approach for multi-user UWB communications," *IEEE Trans. Antennas Propagat.*, submitted for publication.

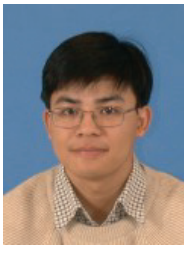

**Hung Tuan Nguyen** (S'03) received the BSc.E.E. in Electronic Engineering from Hanoi University of Technology Vietnam in 1999. In 2002 he obtained the MSc.E.E. in Telecommunication from the Technical University of Denmark. In 2005 he got the PhD degree from Aalborg University, Denmark. He is now working as a researcher at the Department Communication Technology, Aalborg University. His interest lies in MIMO radio channel modelling and characterizations, transmission techniques for multiple antennas system and studying the applicability of multiple antenna system in a small terminal.

**Jørgen Bach Andersen** (M'68-SM'78-F'92) received the M.Sc. and dr.techn. degrees from the Technical University of Denmark (DTU), Lyngby, Denmark, in 1961 and 1971, respectively. In 2003 he was awarded an honorary degree from Lund University, Sweden. From 1961 to 1973, he was with the Electromagnetics Institute, DTU, and since 1973 he has been with Aalborg University, Aalborg, Denmark, where he is now a Professor Emeritus. He has been a Visiting Professor in Tucson, Arizona, Christchurch, New Zealand, Vienna, Austria, and Lund, Sweden. From 1993-2003, he was Head of the Center for Personkommunikation (CPK), dealing with modern wireless communications. He has published widely on antennas, radio wave propagation, and communications, and has also worked on biological effects of electromagnetic systems. He was on the management committee for COST 231 and 259, a collaborative European program on mobile communications. He has recently published a popular monograph, "Channels, Propagation and Antennas for Mobile Communications," together with Prof. R. G. Vaughan.

Professor Andersen is a Life Fellow of IEEE and a former Vice President of the International Union of Radio Science (URSI) from which he was awarded the John Howard Dellinger Gold Medal in 2005.

**Gert Frølund Pedersen** received the B.Sc. E. E. degree, with honour, in electrical engineering from College of Technology in Dublin, Ireland in 1991, and the M.Sc. E. E. degree and Ph. D. from Aalborg University in 1993 and 2003. He has been with Aalborg University since 1993 where he currently is working as Professor in the Antenna and propagation group. His research has focused on radio communication for mobile terminals including small antennas, antenna-systems, propagation and biological effects and has more than 100 publications including more than 10 patents. He has also worked as consultant in small antennas and developed more than 50 dedicated designs for mobile terminals starting with the first internal antenna for mobile phones in 1993 with very low SAR, First internal triple-band antenna in 1998 with low SAR and high efficiency and various antenna diversity systems rated as the most efficient on the market. Recently he has been involved in establishing a method to measure the communication performance for mobile terminals that can be used as a basis for a 3G standard where measurements also including the antenna will be needed. Further he is involved in small terminals for 4G including several antennas (MIMO systems) and ultra wide band antennas to enhance the data communication.

**Persefoni Kyritsi** (S'98-M'02) received the B.S. degree in electrical engineering from the National Technical University of Athens, Athens, Greece, in 1996, the M.S. and the Ph.D. degrees in Electrical Engineering from Stanford University, Stanford, CA, in 1998 and 2002 respectively. She has spent time as an intern with Lucent Technologies Bell Labs, Deutsche Telekom, Intel and Nokia. During the period September 2003 to August 2005, she was with the Department of Mathematics at Stanford University as a visiting researcher. Since 2001, she has been with the Department Communication Technology in Aalborg University, Aalborg, Denmark, where she currently holds the position of Assistant Professor. Her research interests include radio propagation, multiple antenna systems, time reversal communications, cooperative wireless techniques and cross-layer issues.

**Patrick Claus Friedrich Eggers** (M.Sc.E.E., PhD) (M'91) Associate Professor, has since 1992 been project leader of the propagation group of CPK. He is now the research coordinator of the Antennas and Propagation division, Department of Communication Technology (KOM), Aalborg University (AAU). He is on the technical research council of the Center for TeleInFrastruktur (CTIF) at AAU, and has been project and work package manager in several European research projects (TSUNAMI, CELLO etc) and in industrial projects with partners as Nokia, Ericsson, Motorola, IOSpan, ArrayComm, Avendo Wireless, Samsung etc., as representative of CTIF, KOM (and previously the center for PersonKommunikation-CPK). He is author of over 40 papers, as well as section author and chapter editor in different COST final reports (COST207, 231, 259) and books on ultra wideband and cooperative communication. He is initiator and coordinator of an internationally targeted M.Sc.E.E. program in Mobile Communications taught in English at Aalborg University, as well as designer and coordinator of the newly started programme in Software Defined Radio.